PHYSICAL REVIEW A **87**, 041604(R) (2013)

Strongly interacting array of Bose-Einstein condensates trapped in a one-dimensional optical lattice

Makoto Yamashita,[1,2] Shinya Kato,[2,3] Atsushi Yamaguchi,[2,4] Seiji Sugawa,[2,3] Takeshi Fukuhara,[3]
Satoshi Uetake,[2,3] and Yoshiro Takahashi[2,3]

[1]*NTT Basic Research Laboratories, NTT Corporation, 3-1 Morinosato-Wakamiya, Atsugi-shi, Kanagawa 243-0198, Japan*
[2]*Japan Science and Technology Agency, CREST, 5 Sanbancho, Chiyoda-ku, Tokyo 102-0075, Japan*
[3]*Department of Physics, Graduate School of Science, Kyoto University, Kyoto 606-8502, Japan*
[4]*National Institute of Information and Communications Technology, 4-2-1, Nukui-Kitamachi, Koganei, Tokyo 184-8795, Japan*

(Received 27 August 2011; published 29 April 2013)

We study a strongly interacting array of Bose-Einstein condensates trapped in a one-dimensional (1D) optical lattice. The system is described by a nonstandard 1D Bose-Hubbard model in which both the tunneling matrix element and the on-site atomic interaction depend on the lattice site due to the interaction broadening of the local wave function and the system inhomogeneity. We quantitatively compare theoretical analyses based on the Gutzwiller approximation with experimental observations obtained using ytterbium atoms. We show that atomic states are highly number squeezed owing to strong interatomic interactions as the lattice potential becomes deeper. Furthermore, the calculated inhomogeneous collisional broadening of spectroscopic line shapes agrees well with high-resolution spectra measured by using the ultranarrow magnetic quadrupole $^1S_0$-$^3P_2$ transition.

DOI: 10.1103/PhysRevA.87.041604 PACS number(s): 03.75.Lm, 67.85.Hj, 37.10.Jk, 03.75.Hh

The realization of Bose-Einstein condensation in ultracold atomic gases has opened the way to highly accurate interferometric measurements based on atomic de Broglie waves [1]. From our knowledge of quantum optics, we can expect that the employment of quantum strategies such as squeezing and entanglement will greatly improve the sensitivity of interferometry below the standard quantum limit, namely, quantum metrology [2]. Advanced atom-manipulation techniques have led to the successful generation of squeezed states of atoms using optical lattices [3–11]. The role of interatomic interaction in generating a nonclassical atomic state, however, remains not fully understood so far both in theory and experiment. Important recent theoretical progress reveals a breakdown of the standard Bose-Hubbard model to describe a strongly interacting Bose gas in an optical lattice [12–17]. This suggests that the squeezing property of atoms is determined by the highly complicated processes. Precise studies of the many-body atomic states, especially the detailed behaviors of a crossover from a superfluid to a squeezed state, are therefore essential for developing quantum metrology with ultracold atoms.

In this Rapid Communication, we provide a systematic study on a strongly interacting array of Bose-Einstein condensates (BEC) trapped in a one-dimensional (1D) optical lattice. A combination of theoretical analysis based on a nonstandard 1D Bose-Hubbard (BH) model [12–17] with harmonic confining potential and experimental measurements both for the matter wave interference and also high-resolution spectroscopy on density-dependent collisional frequency shifts enables us to quantitatively clarify the details of crossover from a superfluid to a highly number-squeezed state. In particular, this work sheds light on the important role of the interatomic interactions in significantly modifying the Wannier function and therefore the Hubbard parameters.

We begin by describing the experimental setup that characterizes our present system. Condensates of ytterbium (^{174}Yb) are trapped optically using far-off-resonance trap (FORT) laser beams [18]. The configuration of vertical and horizontal FORT lasers results in a three-dimensional (3D) harmonic confining potential given by $V_{\rm trap}(x,y,z) = m(\omega_x^2 x^2 + \omega_y^2 y^2 + \omega_z^2 z^2)/2$, where m is the mass of Yb atoms and ω_α ($\alpha = x,y,z$) is the trapping frequency along the α direction. A lattice laser is then applied along the z axis and produces a 1D optical lattice potential here given by $V_{\rm lat}(z) = V_0 \sin^2(2\pi z/\lambda)$, where V_0 is the depth of lattice potential and λ (=532 nm) is the laser wavelength. This lattice potential produces a significantly tighter confinement than a harmonic potential: The trapping frequency of lattice, $\omega_{\rm lattice} = (2\pi/\lambda)\sqrt{2V_0/m}$, satisfies the relation $\omega_{\rm lattice} \gg \omega_\alpha$. The system can be considered as an array of quasi-two-dimensional (2D) pancake-shaped condensates aligned along the z axis [19].

Note that $\hbar\omega_{\rm lattice}$ is much larger than other energy scales characterizing an individual pancake condensate at each site: $\hbar\omega_x$, $\hbar\omega_y$, and the mean-field interaction energy. Thus, the normalized local wave function of a condensate at the ith site can be factorized as $\Phi_i(x,y,z) = \psi_i(x,y)\, w(z - z_i)$, where $w(z - z_i)$ represents the Wannier function at the site of z_i. We obtain $w(z)$ numerically via the Bloch functions in the *ab initio* manner as a function of lattice depth $s = V_0/E_{\rm r}$, where $E_{\rm r} = h^2/(2m\lambda^2)$ is the recoil energy and h is Planck's constant. The wave function $\psi_i(x,y)$ with the fixed atom number in the absence of tunneling approximately obeys the following 2D Gross-Pitaevskii (GP) equation [20]:

$$-\frac{\hbar^2}{2m}\left(\nabla_x^2 + \nabla_y^2\right)\psi_i(x,y) + \frac{m}{2}\left(\omega_x^2 x^2 + \omega_y^2 y^2\right)\psi_i(x,y) + g'\bar{n}_i|\psi_i(x,y)|^2\psi_i(x,y) = \mu_i\psi_i(x,y), \quad (1)$$

where g' is the coupling parameter, $\bar{n}_i$ is the number of condensed atoms at the ith site, and μ_i is the chemical potential. The value of g' is evaluated numerically through the relation $g' = g\int |w(z)|^4\, dz$, where $g = 4\pi\hbar^2 a_{11}/m$ and a_{11} (=5.53 nm) is the s-wave scattering length between the $^1S_0$ ground states of ^{174}Yb atoms [21,22].

The tunneling of atoms between adjacent lattice sites causes certain atom number fluctuations in pancake-shaped condensates. As has been observed experimentally [3,19], the system stays in the superfluid state with large number

 ©2013 American Physical Society

fluctuations if the lattice depth is relatively shallow, while the system moves towards the number-squeezed state with reduced number fluctuations as the lattice depth increases. To analyze this property quantitatively, we introduce a nonstandard 1D BH model described by the following Hamiltonian [12–17]:

$$\hat{H} = -\sum_{\langle i,j\rangle} J_{i,j}(\hat{a}_i^\dagger \hat{a}_j + \text{H.c.}) + \frac{1}{2}\sum_i U_i \hat{n}_i(\hat{n}_i - 1) + \sum_i \epsilon_i \hat{n}_i, \quad (2)$$

where $\hat{a}_i^\dagger$ ($\hat{a}_i$) is the creation (annihilation) operator for bosons at the ith lattice site, and $\hat{n}_i$ ($=\hat{a}_i^\dagger \hat{a}_i$) is the local number operator. The abbreviation $\langle i,j\rangle$ in the hopping term represents a summation over adjacent sites and ϵ_i is the energy offset at the ith site caused by the harmonic confining potential along the z axis, i.e., $\epsilon_i = m\omega_z^2\lambda^2 i^2/8$.

Both the repulsive on-site interaction U_i and the tunneling matrix element $J_{i,j}$ depend on the filling, which in turn depends on the lattice site. This feature significantly differs from the conventional BH Hamiltonian and reflects the fact that the local wave function Φ_i is broadened in the xy plane perpendicular to the 1D optical lattice leading to a renormalization of both U_i and $J_{i,j}$. We evaluate these renormalized model parameters [12–17]:

$$U_i = g\int dx\,dy\,dz|\Phi_i|^4 = g'\int dx\,dy|\psi_i(x,y)|^4 \quad (3)$$

and

$$J_{i,j} = \int dx\,dy\,dz\,\Phi_i^*\left\{-\frac{\hbar^2}{2m}\nabla_z^2 + V_{\text{lat}}(z)\right\}\Phi_j, \approx J\int dx\,dy\,\psi_i^*(x,y)\psi_j(x,y), \quad (4)$$

where J is the tunneling matrix element along the 1D lattice obtained numerically through the width of the lowest Bloch band. Here we assume ψ_i to be the ground-state wave function for the GP equation in Eq. (1) and neglect the effects of collective excitations in each pancake condensate. U_i is determined self-consistently as a functional of $\bar{n}_i$ under the condition that $\bar{n}_i$ in Eq. (1) is equal to the expectation value of the local number operator included in the Hamiltonian, i.e., $\bar{n}_i = \langle\hat{n}_i\rangle$. $J_{i,j}$ is evaluated similarly as a functional of both $\bar{n}_i$ and $\bar{n}_j$.

The ground-state property of the Hamiltonian in Eq. (2) is investigated numerically based on the Gutzwiller approximation. We employ the highly efficient numerical method based on iteration in imaginary time developed in Ref. [23]. In this method, the ground state is obtained by imposing a convergence criterion for high numerical precision. It is also noted that, at each iteration step, we calculate the renormalized parameters U_i and $J_{i,j}$ using Eqs. (1), (3), and (4) associated with given expectation values of local number operators $\bar{n}_i^{(k)}$, where the suffix k represents the number of iterations.

Figure 1 shows the average number of atoms $\bar{n}_i = \langle\hat{n}_i\rangle$ and the number variance $\Delta_i = \langle\hat{n}_i^2\rangle - \bar{n}_i^2$ over the lattice sites for the four different depths of optical lattice potential. We choose the parameters relevant to the experiments: (a) $s = 5$ and $(\omega_x,\omega_y) = 2\pi \times (26,181)$ Hz; (b) $s = 10$ and $(\omega_x,\omega_y) = 2\pi \times (37,183)$ Hz; (c) $s = 15$ and $(\omega_x,\omega_y) = 2\pi \times (46,185)$ Hz; (d) $s = 25$ and $(\omega_x,\omega_y) = 2\pi \times (59,189)$ Hz. For all four cases, we further assume $\omega_z = 2\pi \times 147$ Hz, the total number of Yb atoms $N \simeq 1.5 \times 10^4$, and the number of lattice sites $M = 41$. From the histograms in Fig. 1, Yb atoms are smoothly distributed over about 20 lattice sites and there are more than 1 400 atoms at the central site. The spatial distribution of the atoms spreads as s increases, which originates from the fact that the interaction becomes stronger in the deeper optical lattice with a tight confinement.

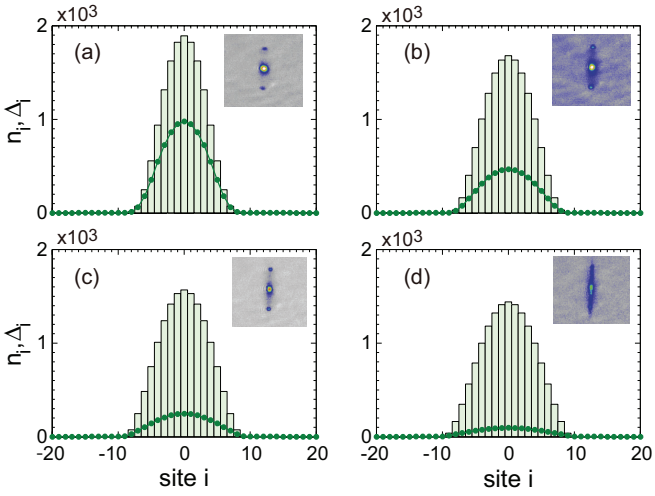

FIG. 1. (Color online) Calculated results on the average number of atoms $\bar{n}_i$ (histograms) and the profiles of number variance Δ_i (circles) for the four different lattice depths relevant to the experiments: (a) $s = 5$, (b) $s = 10$, (c) $s = 15$, and (d) $s = 25$. Insets are experimentally observed time-of-flight images.

A Gutzwiller analysis allows us to study the local number fluctuations caused by the tunneling of atoms. The solid circles in Fig. 1 show the profiles of the number variance Δ_i corresponding to the four different lattice depths. The local number fluctuations are significantly suppressed owing to strong interactions as the lattice depth increases, namely, the atoms are number squeezed. Here we discuss such a squeezing property of our present system more systematically by introducing a squeezing factor defined by $S_q = -10\log_{10}(\Delta_i/\bar{n}_i)$ [3,24]. Note that this factor depends on the lattice site owing to the inhomogeneity caused by the harmonic confining potential along the lattice direction. At the central site, for instance, we obtain the following squeezing factors for four different lattice depths: $S_q = 2.9$ dB for $s = 5$, $S_q = 5.6$ dB for $s = 10$, $S_q = 8.1$ dB for $s = 15$, and $S_q = 11.8$ dB for $s = 25$. A highly number-squeezed state has been achieved in the deepest optical lattice. We did not observe any interference patterns in the time-of-flight image as shown by the inset in Fig. 1(d), whereas in the insets of Figs. 1(a)–1(c) interference fringes are clearly shown, which is consistent with the calculated number variances and squeezing parameters. Furthermore, we confirmed that the above S_q values are quite consistent with the previous results measured by Orzel *et al.* in Ref. [3] [25].

Next we briefly explain how the Hubbard parameters are modified in the calculations. Figure 2 shows the site dependence of these renormalized parameters for the shallowest lattice depth with $s = 5$ corresponding to Fig. 1(a). In Fig. 2(a),

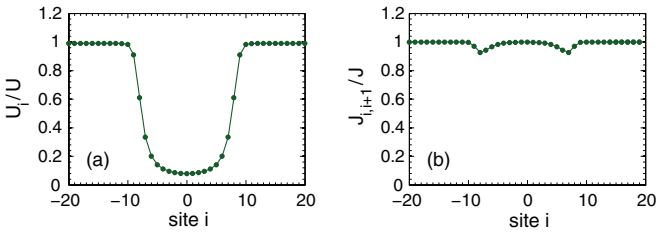

FIG. 2. (Color online) Calculated results on the site dependence of renormalized parameters (a) U_i and (b) $J_{i,i+1}$ for the lattice with $s = 5$. The parameters are fixed as in Fig. 1(a).

we plot U_i in units of the value without interaction broadening, i.e., $U = (g'm/h)\sqrt{\omega_x\omega_y}$. The U_i values decrease greatly at the sites around the center, where $\bar{n}_i$ is large, through the significant broadening of local wave functions $\psi_i(x,y)$ satisfying Eq. (1) [12–17], while they are fixed at $U_i = U$ at the low filling sites. On the other hand, in Fig. 2(b), the tunneling matrix element $J_{i,i+1}$ is slightly reduced near the edges of atom distribution along the lattice (i.e., around $i = \pm 7$) as a result of the fact that the overlap of local wave functions between the adjacent sites decreases there from Eq. (4). The features shown in Fig. 2 are almost the same for other deeper lattices and the renormalization of U_i plays a dominant role in the present system.

A series of experiments have demonstrated that high-resolution spectroscopy is a powerful tool for exploring the many-body effects in quantum degenerate atomic gases [26–30]. The density-dependent collisional frequency shift in the excitation process provides us with important information about the mean-field energy of interacting atoms. In this respect, two-electron atoms of Yb [31] possess very attractive properties. Their ultranarrow optical transitions including the so-called "clock transition" make them an extremely highly sensitive probe for the collisional frequency shift [18,32,33]. To clarify the role of interatomic interactions in the present system in more detail, high-resolution spectroscopy utilizing the ultranarrow $^1S_0$-$^3P_2$ transition of ^{174}Yb atoms [18] has been performed under weak excitation conditions such that at most 600 atoms are excited among a total of 1.5×10^4 atoms.

The solid circles in Fig. 3 correspond to the experimentally measured spectra for the four different lattice depths. Here the zero-frequency offset is defined by the probe laser frequency at the maximum point of the measured spectrum in Fig. 3(a). The vertical axis corresponds to the fluorescence signal detected on a CCD camera. We see that the spectrum moves towards the lower frequency region from Figs. 3(a) to 3(d) according to the different Stark shift of the excited $^3P_2$ state with a different FORT potential that depends on the lattice depth. More importantly, all the measured spectra shown in Fig. 3 are very broad. Furthermore, as the optical lattice deepens, the spectral width gradually increases and the spectral peak height decreases correspondingly. This feature cannot be simply explained by the following experimental factors that contribute to the broadening of the spectra. The natural linewidth of the $^1S_0$-$^3P_2$ transition is about 10 mHz. The frequency resolution of the probe laser is about 1 kHz. In addition, there is an inhomogeneous Stark shift caused by the optical lattice potential because the wavelength of the present lattice laser

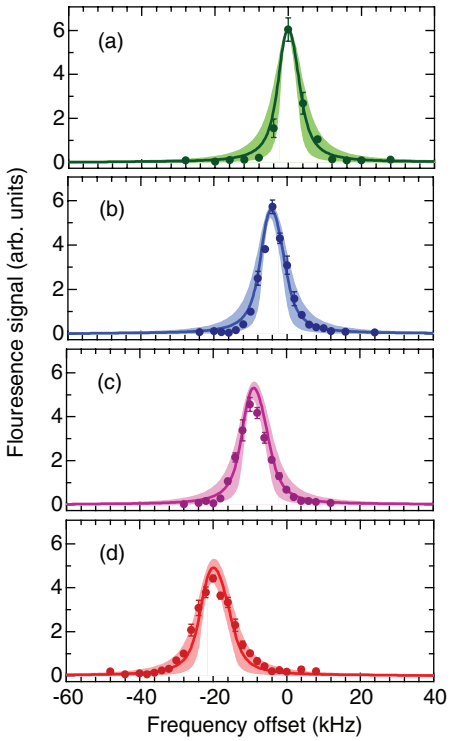

FIG. 3. (Color online) High-resolution spectra using ultranarrow $^1S_0$-$^3P_2$ transition of ^{174}Yb atoms for four different lattice depths: (a) $s = 5$, (b) $s = 10$, (c) $s = 15$, and (d) $s = 25$. The solid circles correspond to the measured spectra and the solid lines correspond to the calculated spectroscopic line shapes based on Eq. (5) with the spectral broadening of $\delta = 2.5$ kHz. The shaded areas along the solid lines represent the numerical results when δ changes from 1 to 4 kHz. The error bars represent the standard deviation of the measurements.

deviates slightly from the *magic wavelength* for Yb atoms [18]. We estimate the value of this inhomogeneous Stark shift to be about 2 kHz in the present experiments. The measured spectral width exceeds 10 kHz and this clearly exceeds the broadening that originated from these experimental factors.

We analyze these measured spectra numerically [23,34,35] on the basis of inhomogeneous spectral broadening induced by atomic interactions [26–30]. In the limit of weak excitation, the density-dependent collisional frequency shift at the ith lattice site $\Delta\nu_i$ is given locally by $\Delta\nu_i(x,y) = G^{(2)}\Delta a\, g'\bar{n}_i\, |\psi_i(x,y)|^2/(a_{11}h)$, where $\Delta a = a_{12} - a_{11}$, and $a_{12} = -23$ nm [18] is the s-wave scattering length between the $^1S_0$ ground state and the $^3P_2$ excited state of ^{174}Yb atoms. Thanks to the relatively large a_{12} in comparison with that of alkali-metal atoms, the collisional frequency shift of Yb becomes detectable in the optical frequency region. $G^{(2)}$ is a two-particle correlation function at zero distance and we assume $G^{(2)} = 1$ for indistinguishable bosonic ^{174}Yb atoms. Note that, in the above expression of $\Delta\nu_i$, we average out the contribution along the z axis with the tight confinement of the lattice potential. A normalized spectroscopic line shape is then introduced as a function of frequency offset ν:

$$I(\nu - \nu_0) = \frac{1}{N}\sum_i \int dx\, dy \frac{1}{\pi} \frac{\delta\bar{n}_i |\psi_i(x,y)|^2}{\{\Delta\nu_i(x,y) - \nu + \nu_0\}^2 + \delta^2}, \quad (5)$$

where ν_0 is the origin of the frequency offset, and δ in a Lorentzian form [36] corresponds to the spectral broadening that originated from the several experimental factors mentioned above. The dominant factor in our experiment is the inhomogeneous Stark shift caused by the optical lattices, and we choose $\delta = 2.5$ kHz. This line shape is highly sensitive to the many-body ground state of the present system via the collisional frequency shift.

The calculated line shapes using $\delta = 2.5$ kHz are plotted with solid lines in Fig. 3, accompanied by the shaded areas that represent the results when δ changes from 1 to 4 kHz for comparison. Here we reasonably assume that the measured weak excitation spectra are proportional to the normalized spectroscopic line shape of Eq. (5) irrespective of lattice depth. We determine the proportionality coefficient α and the value of ν_0 such that, for the shallowest lattice with $s = 5$, the peak value of $\alpha I(\nu - \nu_0)$ fits the maximum point of the measured spectrum as shown in Fig. 3(a). For other lattice depths [Figs. 3(b)–3(d)], we use the same α and take account of the influence of different Stark shifts, which leads to a corresponding shift of ν_0. Figure 3 demonstrates that the solid lines reproduce the experimental observations for all four lattice depths regarding both the spectral widths and spectral peak heights without any fitting parameters. We have shown that the measured broad high-resolution spectra can be quantitatively explained by the density-dependent collisional broadening.

In summary, we have studied both theoretically and experimentally a strongly interacting array of BECs trapped in a 1D optical lattice. We analyzed the number-squeezing property by introducing a nonstandard 1D BH model that successfully includes the effect of the broadening of local wave functions owing to repulsive interatomic interactions. The measured high-resolution spectra obtained using the ultranarrow $^1S_0$-$^3P_2$ transition agree quantitatively with theoretical simulations that carefully deal with the density-dependent large collisional frequency shift of Yb atoms. Interesting future work will involve applying the present high-resolution spectroscopy to Yb condensates trapped in a 3D optical lattice [37], which will allow us to investigate precisely the quantum phase transition from a superfluid to a Mott insulator.

We thank K. Inaba, K. Shibata, R. Yamamoto, Y. Yoshikawa, D. Hashimoto, K. Igeta, and Y. Tokura for valuable discussions. This work was partially supported by the Grant-in-Aid for Scientific Research of JSPS [No. 21102005C01 (Quantum Cybernetics), No. 22244050, and No. 23654086], GCOE Program "The Next Generation of Physics, Spun from Universality and Emergence" from MEXT of Japan, and FIRST.

[1] For a review, see K. Southwell, Nature (London) **416**, 205 (2002).
[2] V. Giovannetti, S. Lloyd, and L. Maccone, Science **306**, 1330 (2004).
[3] C. Orzel, A. K. Tuchman, M. L. Fenselau, M. Yasuda, and M. A. Kasevich, Science **291**, 2386 (2001).
[4] M. Greiner, O. Mandel, T. Esslinger, T. W. Hänsch, and I. Bloch, Nature (London) **415**, 39 (2002).
[5] F. Gerbier, S. Fölling, A. Widera, O. Mandel, and I. Bloch, Phys. Rev. Lett. **96**, 090401 (2006).
[6] W. Li, A. K. Tuchman, H.-C. Chien, and M. A. Kasevich, Phys. Rev. Lett. **98**, 040402 (2007).
[7] J. Estève, C. Gross, A. Weller, S. Giovanazzi, and M. K. Oberthaler, Nature (London) **455**, 1216 (2008).
[8] A. K. Tuchman and M. A. Kasevich, Phys. Rev. Lett. **103**, 130403 (2009).
[9] C. Gross, T. Zibold, E. Nicklas, J. Estève, and M. K. Oberthaler, Nature (London) **464**, 1165 (2010).
[10] A. Itah, H. Veksler, O. Lahav, A. Blumkin, C. Moreno, C. Gordon, and J. Steinhauer, Phys. Rev. Lett. **104**, 113001 (2010).
[11] C. Gross, J. Estève, M. K. Oberthaler, A. D. Martin, and J. Ruostekoski, Phys. Rev. A **84**, 011609(R) (2011).
[12] D. van Oosten, P. van der Straten, and H. T. C. Stoof, Phys. Rev. A **67**, 033606 (2003).
[13] O. E. Alon, A. I. Streltsov, and L. S. Cederbaum, Phys. Rev. Lett. **95**, 030405 (2005).
[14] A. K. Tuchman, C. Orzel, A. Polkovnikov, and M. A. Kasevich, Phys. Rev. A **74**, 051601(R) (2006).
[15] J. Li, Y. Yu, A. M. Dudarev, and Q. Niu, New J. Phys. **8**, 154 (2006).
[16] D.-S. Lühmann, K. Bongs, K. Sengstock, and D. Pfannkuche, Phys. Rev. Lett. **101**, 050402 (2008).
[17] O. Dutta, A. Eckardt, P. Hauke, B. Malomed, and M. Lewenstein, New J. Phys. **13**, 023019 (2011).
[18] A. Yamaguchi, S. Uetake, S. Kato, H. Ito, and Y. Takahashi, New J. Phys. **12**, 103001 (2010).
[19] P. Pedri, L. Pitaevskii, S. Stringari, C. Fort, S. Burger, F. S. Cataliotti, P. Maddaloni, F. Minardi, and M. Inguscio, Phys. Rev. Lett. **87**, 220401 (2001).
[20] M. D. Lee, S. A. Morgan, M. J. Davis, and K. Burnett, Phys. Rev. A **65**, 043617 (2002).
[21] K. Enomoto, M. Kitagawa, K. Kasa, S. Tojo, and Y. Takahashi, Phys. Rev. Lett. **98**, 203201 (2007).
[22] M. Kitagawa, K. Enomoto, K. Kasa, Y. Takahashi, R. Ciurylo, P. Naidon, and P. S. Julienne, Phys. Rev. A **77**, 012719 (2008).
[23] M. Yamashita and M. W. Jack, Phys. Rev. A **79**, 023609 (2009); **76**, 023606 (2007).
[24] J. Javanainen, Phys. Rev. A **60**, 4902 (1999).
[25] It is noted that the ratio $\bar{n}_i U_i / J_{i,i+1}$ in our calculation is equivalent to the control parameter $Ng\beta/\gamma$ used in Ref. [3]. For comparison, we calculate the values of $\bar{n}_i U_i / J_{i,i+1}$ at the central site: 2.72 for $s = 5$, 11.9 for $s = 10$, 40.3 for $s = 15$, and 299 for $s = 25$.
[26] T. C. Killian, D. G. Fried, L. Willmann, D. Landhuis, S. C. Moss, T. J. Greytak, and D. Kleppner, Phys. Rev. Lett. **81**, 3807 (1998).
[27] J. Stenger, S. Inouye, A. P. Chikkatur, D. M. Stamper-Kurn, D. E. Pritchard, and W. Ketterle, Phys. Rev. Lett. **82**, 4569 (1999).

[28] D. M. Harber, H. J. Lewandowski, J. M. McGuirk, and E. A. Cornell, Phys. Rev. A **66**, 053616 (2002).

[29] A. Görlitz, T. L. Gustavson, A. E. Leanhardt, R. Löw, A. P. Chikkatur, S. Gupta, S. Inouye, D. E. Pritchard, and W. Ketterle, Phys. Rev. Lett. **90**, 090401 (2003).

[30] G. K. Campbell, J. Mun, M. Boyd, P. Medley, A. E. Leanhardt, L. G. Marcassa, D. E. Pritchard, and W. Ketterle, Science **313**, 649 (2006).

[31] Y. Takasu, K. Maki, K. Komori, T. Takano, K. Honda, M. Kumakura, T. Yabuzaki, and Y. Takahashi, Phys. Rev. Lett. **91**, 040404 (2003).

[32] S. Uetake, A. Yamaguchi, D. Hashimoto, and Y. Takahashi, Appl. Phys. B **93**, 409 (2008).

[33] G. K. Campbell, M. M. Boyd, J. W. Thomsen, M. J. Martin, S. Blatt, M. D. Swallows, T. L. Nicholson, T. Fortier, C. W. Oates, S. A. Diddams, P. Naidon, P. Julienne, J. Ye, and A. D. Ludlow, Science **324**, 360 (2009).

[34] K. R. A. Hazzard and E. J. Mueller, Phys. Rev. A **76**, 063612 (2007).

[35] K. R. A. Hazzard and E. J. Mueller, Phys. Rev. A **81**, 033404 (2010).

[36] As discussed in Ref. [35], locally there could be a spectral structure beyond a simple peak that is smeared out when considering the full trapped system.

[37] T. Fukuhara, S. Sugawa, M. Sugimoto, S. Taie, and Y. Takahashi, Phys. Rev. A **79**, 041604(R) (2009).